PROCEEDINGS OF SCIENCE

High Energy Sources Monitored with OMC

D. Risquez[*†]
Centro de Astrobiología – LAEFF (CSIC–INTA), Spain
E-mail: risquez@strw.leidenuniv.nl

A. Domingo
Centro de Astrobiología – LAEFF (CSIC–INTA), Spain
E-mail: albert@laeff.inta.es

M.D. Caballero-García[‡]
Centro de Astrobiología – LAEFF (CSIC–INTA), Spain
E-mail: mcaballe@ast.cam.ac.uk

J. Alfonso-Garzón
Centro de Astrobiología – LAEFF (CSIC–INTA), Spain
E-mail: julia@laeff.inta.es

J.M. Mas-Hesse
Centro de Astrobiología – LAEFF (CSIC–INTA), Spain
E-mail: mm@laeff.inta.es

During the last five years, the Optical Monitoring Camera (OMC) on-board *INTEGRAL* has been observing the optical counterparts of high energy sources. In this contribution we present the results for some of the most interesting sources analyzed up to now, mostly X-ray binary systems, discussing the correlation between the optical and the high energy (X and gamma-rays) emission. We also describe the capabilities of the OMC Data Center at http://sdc.laeff.inta.es/omc, from which all optical light curves obtained by OMC can be previewed and easily downloaded. In this paper we present the light curves of the X-ray binaries: Cyg X–1, GX 301–02, Sco X–1, SS Cyg, LSI +61°303, and Her X–1.

7th INTEGRAL *Workshop*
September 8-11 2008
Copenhagen, Denmark

*Speaker.
†Currently at Leiden Observatory (The Netherlands)
‡Currently at Institute of Astronomy (Cambridge, UK)

PoS(Integral08)129

1. Introduction

The *INTEGRAL* Optical Monitoring Camera, OMC (Mas-Hesse et al. 2003), observes the optical emission from the prime targets of the gamma-ray instruments on-board the ESA mission *INTEGRAL*: SPI (gamma-ray spectrometer) and IBIS (gamma-ray imager), with the support of the JEM-X monitor in the X-ray domain. OMC has its field of view (FOV) almost coinciding with the fully coded FOV of JEM-X, and it is co-aligned with the central part of the larger fields of view of IBIS and SPI. This capability provides invaluable diagnostic information on the nature and the physics of the sources over a broad wavelength range.

OMC is based on a refractive optics with a Johnson V filter pass band (centred at 550 nm). It has an aperture of 50 mm focused onto a large format CCD (1024×2048 pixels) working in a frame transfer mode (1024×1024 pixels imaging area). Its field of view is $5^\circ \times 5^\circ$ and image scale is 17.5 arcsec/pixel. The point spread function is a Gaussian with FWHM (Full Width at Half Maximum) $\simeq 1.3$ pixels ($\simeq 23$ arcsec). Point source location accuracy is around 2 arcsec (1σ).

It works properly within a 10^4 flux factor dynamic range, from $V \simeq 7$ mag (saturation effects appears) to $V \approx 16-17$ mag (magnitude limit for 3σ source detection, combining all shots per pointing). This magnitude limit depends on the sky background and source contamination, which can be very important. OMC single shots have variable exposure. Currently it is performing a 10, 50, and 200 seconds exposures cycle.

Due to telemetry restrictions, only a fraction of the CCD image is transmitted to Earth, usually 1% of its pixels. Several subwindows (typically 100, and in any case less than 228) of 11×11 pixels are extracted and sent to ground. The targets to be monitored have to be preselected on ground. For this purpose, an OMC Input Catalogue (Domingo et al. 2003) was compiled. It contains most gamma and X-ray sources, variable stars, and HIPPARCOS and Tycho reference stars for astrometric and photometric calibration. The Catalogue contains currently more than 500 000 targets.

Fluxes are calculated in three different nearly circular apertures: 1, 3, and 5 pixel diameter. Absolute photometric calibration is achieved by comparison with a number of standard reference stars within the field of view of the instrument. In the long term, good targets have single photometric points with an absolute photometric accuracy of about 0.02 mag (1σ).

After the proprietary period of one year, all *INTEGRAL* data are open to the scientific community. The OMC team has developed a scientific archive, containing the data generated by the OMC and an access system capable of performing complex searches, complementary to the *INTEGRAL* Archive hosted at ISDC[1]. The OMC archive is optimised for the optical data.

2. Some Monitored Sources

In this section we show some results obtained using OMC. We take advantage of the simultaneous observation in optical and high energies. The analysis of simultaneous optical/X-ray light curves helps to understand the geometry of the emitting regions, constraining the physical models.

[1] `http://isdc.unige.ch`

PoS(Integral08)129

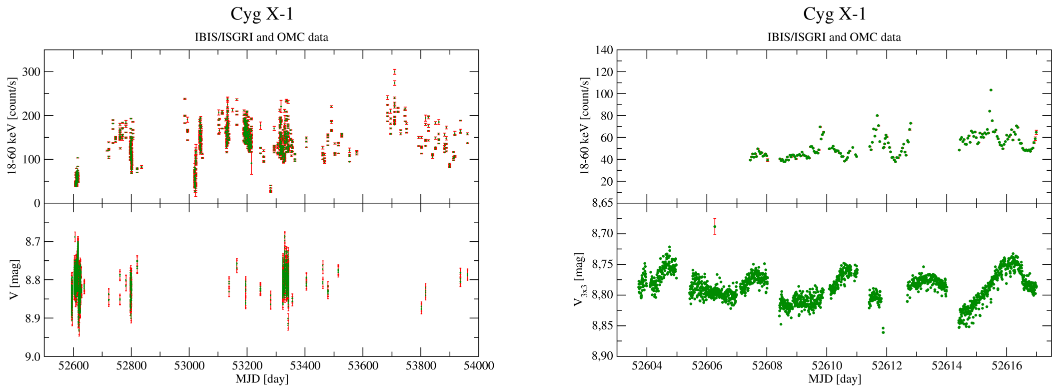

Figure 1: Cyg X–1. On the left we present the complete light curve (up to September/2006), on the right we display a zoom focused on two consecutive orbital periods. In both cases, hard X-rays are in the top and optical light curves in the bottom panel. The variability in the optical band is attributed to the gravitational deformation of the O star. Error bars are included in the plots, except for the optical plot to the right. Note that in this case the error bars are shown in a separated and bogus photometric point.

OMC is very useful for monitoring orbital periods in binary systems, due to its large temporal coverage and the lack of the day-night cycle. These periods are made evident as periodic variations in the optical light curve, usually due to eclipses or tidally deformed stars.

In this paper we use data spanning about 5 years, from the beginning of the mission (October/2002) until October/2007 (depending on the source).

2.1 Cyg X–1

This source is a binary system constituted by an O9.7Iab star and a compact object, potentially a black hole. The optical counterpart is HD 226868 (Bolton 1972; Webster & Murdin 1972).

It is an HMXB (High Mass X-ray Binary), and it is well known that it displays a double-peaked ellipsoidal modulation as expected from a tidally and rotationally distorted star. This tidal distortion is induced by the presence of the massive, though not visible, compact object.

In Fig. 1, left panel, we show simultaneous light curves obtained with IBIS/ISGRI (top) and OMC (bottom). A significant degree of variability, up to 20% in flux peak to peak and with a timescale of hours, is sometimes observed in the OMC data. In the right panel of Fig. 1 there is a zoom of the left plot. The OMC light curve covers two orbital periods (5.599836 ± 0.000024 day, Brocksopp et al. (1999)).

The average amplitude of the optical variations of 0.06 mag, and the difference between maxima of 0.015 mag, confirm earlier studies by Bruevich et al. (1978). Small differences and changes in the light curve probably reflect variations in the activity of the X-ray source. The difference between maxima could be attributed to a non-uniform distribution of the surface brightness of the optical star.

2.2 GX 301–02

This is another HMXB, in this case with a Be super-giant companion (White et al. 1976) and

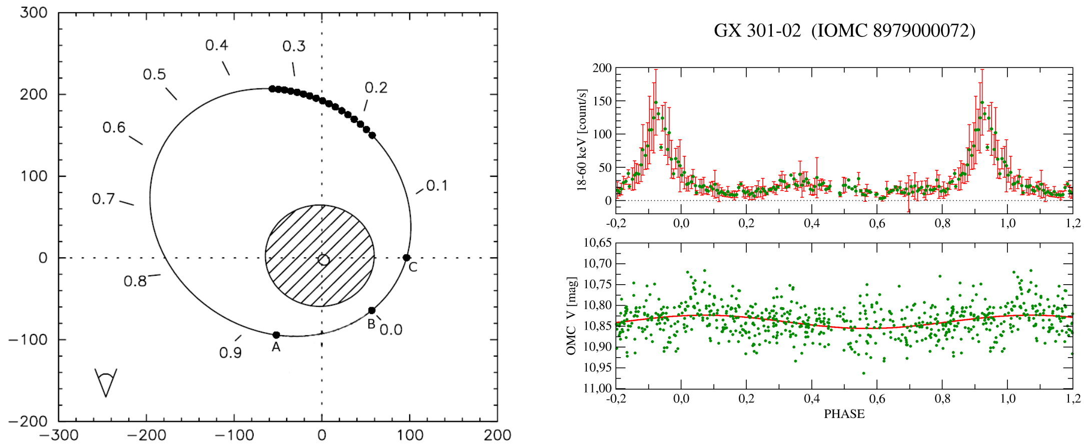

Figure 2: GX 301-02. On the left it is displayed the orbital sketch. It has been modified from Kaper et al. (2006). On the right, the hard X-ray (top) and optical (bottom) light curves folded with the orbital period. The line in the optical plot is a simple sinusoidal fit to the data.

an orbital period of 41.498 days (Bildsten et al. 1997).

In Fig. 2 we use *INTEGRAL* data to justify the physical model of the system. The peak of high energy emission takes place in point A (primary maximum, phase 0.92). Point B is the periastron (phase 0.00 by definition). The peak of optical emission occurs in C (phase 0.07), when the companion star faces the largest cross-section on the line of sight.

The hard X-ray light curve shows two maxima. They happen when the compact object goes through the disc outflow of the super-giant companion, in its orbital movement. Disk density is higher near the super-giant star, and due to that the primary maximum (point A, phase 0.92) is brighter than the secondary one (at phase 0.4, where the disc density is lower). The optical curve shows a weak variability, and it is exactly as expected by the physical model.

2.3 Sco X–1

This source is an LMXB (Low Mass X-ray Binary), also known by its optical counterpart V818 Sco. Its orbital period is very short, 0.787 313 days (Samus et al. 2006).

It is the brightest X-ray extrasolar source as seen from the Earth (*Uhuru* catalog, Giacconi et al. (1972)). The system is composed by a neutron star and a low mass companion ($\sim 1\,M_{\odot}$) which accretes mass via Roche lobe.

It shows a significant level of variability, both at high energies and in the optical band. The histogram of measured magnitudes (see Fig. 3, on the left) shows three clear states of the Sco X–1 optical emission as previously reported (McNamara et al. 2003, 2005; Wright et al. 1975).

2.4 SS Cyg

SS Cyg is a cataclysmic variable constituted by a K4–5 V star filling its Roche lobe which accretes matter on a white dwarf (as disc). The orbital period has been calculated using spectroscopy and it is about 0.275 days (Cowley et al. 1980; Stover et al. 1980).

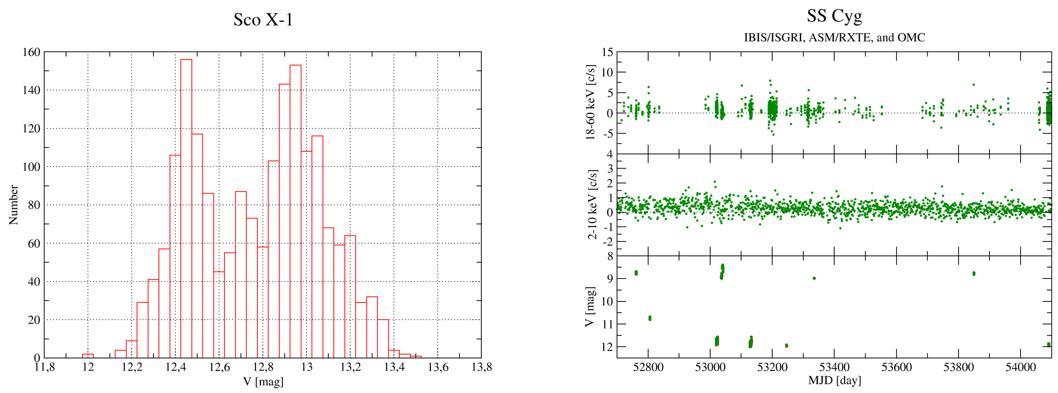

Figure 3: On the left: histogram of magnitudes of Sco X–1. This distribution is characteristic for this source. On the right: SS Cyg light curves. Hard X-ray plot is on top (IBIS/ISGRI), soft X-ray in the middle (ASM/RXTE), and optical light curve by OMC in the bottom.

The light curve (Fig. 3, right panel) shows a high variability in the optical emission, roughly within a factor of 40. However, no trends have been found at high energy, neither any evident correlation between optical and hard X-ray emission.

We also detect variations in magnitude up to 0.1 mag with characteristic times of about 15 minutes. It could be due to a hot spot in the inner part of the disc, near the white dwarf, because the orbital period in the inner part of the accretion disc is much faster than the orbital period of the binary system.

2.5 LSI +61°303

This source is an HMXB, also known as V615 Cas by its optical counterpart. Moreover, radio and TeV gamma-ray emission have been observed from this source (Albert et al. 2008).

The optical emission is clearly variable at long-term (its flux increased by 10% in one year). Erratic variability of hundredths of magnitude at short time scales has been observed (Mendelson & Mazeh 1994). However, it is hardly detected in the hard X-ray domain.

The Scargle periodogram shows several peaks, being more remarkable those at 25.8 days (Paredes et al. 1994) and at 31.4 days. There are other peaks at 202 and 400 days, but they are not significant because of the poor long term observations.

2.6 Her X–1

Her X–1 is an LMXB with a neutron star and a companion star of $2.3\,M_\odot$ circling each other every 1.7 days in an almost circular orbit. X-ray eclipses have been detected when the neutron star is hidden by its companion.

The optical counterpart is also known as HZ Her. Optical variations are due to the tidal distortion of the companion star and the intense X-ray heating of the illuminated face of the companion by the neutron star (Reynolds et al. 1997).

Figure 4, left panel, displays the optical light curve. The insets show an artistic impression of the system and a system sketch during different orbital phases (not to scale and omitting the

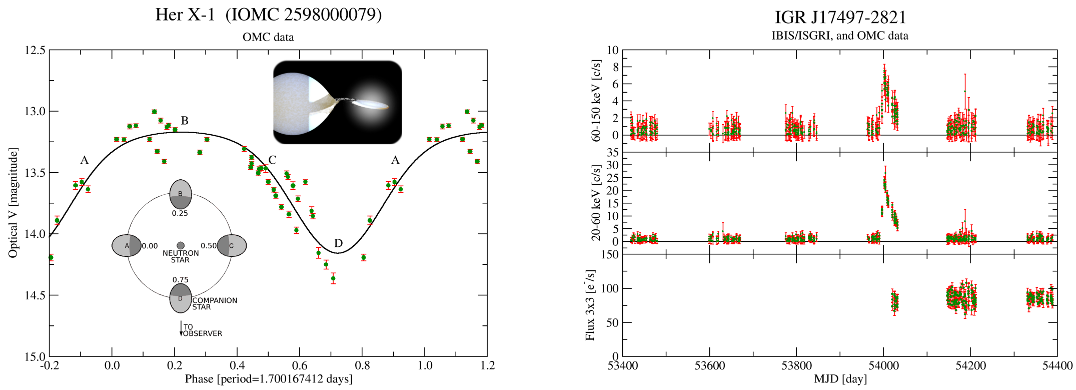

Figure 4: On the left: Her X–1 optical light curve and orbital sketch. On the right: IGR J17497–2821 light curves obtained during the Galactic Bulge Monitoring. Top and middle light curves are in the hard X-ray energy range. The bottom light curve has been obtained with OMC.

accretion disc). Point A (Phase zero by definition, Prince et al. (1994)) corresponds to maximum receding radial velocity. At point B (phase 0.25) we have the maximum of the optical emission, observing the hot face of the X-ray heated optical companion. At point D (phase 0.75) we have the minimum optical emission and we observe the cold face of the companion star and the X-ray eclipse.

3. Galactic Bulge Monitoring

The Galactic Bulge is a region rich in bright variable X-ray and gamma-ray sources. The OMC team is involved in the Galactic Bulge Monitoring (Kuulkers et al. 2007). This project consists in some periodic and systematic observations of this region of the Galaxy with several instruments on-board *INTEGRAL*: IBIS/ISGRI, JEM-X and OMC. The main goal of this monitoring is to obtain simultaneous light curves in different energy ranges. Results (at the moment just for high energies) are publicly available[2].

OMC monitors all sources detected by IBIS/ISGRI in the Galactic Bulge within the FOV of OMC. The full analysis is working in an automatic way, producing the results (light curves) in a short period of time. In this way, if a flare occurs, it could be detected immediately with OMC.

As an example we show IGR J17497–2821 (Fig. 4, right panel). This source was discovered by Soldi et al. (2006). Unfortunately, when the flare was detected OMC was not observing this region. In later observations no significant flux variations have been detected at the position of the source.

4. GRBs

OMC was designed to enter the so-called Trigger Mode if a GRB is detected within its Field of View of $5^\circ \times 5^\circ$. A special software was developed to process this kind of observations. 30 arcmin

[2] `http://isdc.unige.ch/Science/BULGE`

$\times$ 30 arcmin images are taken with 100 seconds of exposure time, and photometry for all sources in the FOV is performed within a very short delay.

According to previous BATSE statistics, around 1 GRB per year was expected within the OMC FOV. Nevertheless, up to now just one GRB took place within OMC, on July 26th, 2005. Unfortunately, it was very close to α Crucis, a very bright star ($V = 0.8$ mag), which saturated completely the CCD and hid the optical counterpart of the GRB.

5. The OMC Archive

The photometrically calibrated light curves produced by OMC (including all sources that have been presented in this work) can be accessed through our web portal[3] (Gutiérrez et al. 2004).

A query form allows to perform complex searches and all optical light curves can be easily previewed and downloaded. The output data may be ordered by object name, coordinates, magnitude, or date and time of observation. The system has a built-in name resolver utility which makes possible to query the archive using any of the objects names provided by SIMBAD. The name resolver gives more than three million and a half identifications for the astronomical objects contained in the OMC catalogue. The full list of the names associated to a given object can be obtained by simply clicking on the target name in the output form.

The archive contains both public and core programme data (which become public after one year) and both types of data can be accessed through the web interface. Currently (October/2008) there are more than 150 000 observed sources in the database, 774 of them having at least 1000 photometric points (combining single shots in 630 second time steps).

A variety of data analysis tools are being developed and will be available in the future. The aim of these tools is to provide added-value functionalities to the system giving the ability to perform data analysis tasks remotely. For example, it is expected to perform time series analysis and light curve characterization using a neural network.

6. Conclusion

OMC obtains photometry using an optical V filter. It allows to perform optical observations simultaneously to high energies ones, using the other instruments on-board *INTEGRAL*. Optical light curves allow us to calculate, for example, orbital characteristics in binary systems.

There is a web page where all OMC data are publicly available. There are data not only of optical counterparts of high energy sources, but also of known optical sources.

The mission is still going on: the database is being increased continuously with both more sources and more photometric points. The Galactic Bulge Monitoring programme is being performed, and OMC is alert to catch future GRBs in its FOV.

Acknowledgment

The activities related to *INTEGRAL*-OMC are being funded since 1993 by the Spanish National Space Programme (MEC/MICINN).

[3] `http://sdc.laeff.inta.es/omc`

References

Albert, J., Aliu, E., Anderhub, H., et al. 2008, ApJ, 684, 1351

Bildsten, L., Chakrabarty, D., Chiu, J., et al. 1997, ApJS, 113, 367

Bolton, C. T. 1972, Nature, 235, 271

Brocksopp, C., Fender, R. P., Larionov, V., et al. 1999, MNRAS, 309, 1063

Bruevich, V. V., Kiliachkov, N. N., Siuniaev, R. A., & Shevchenko, V. S. 1978, Soviet Astronomy Letters, 4, 292

Cowley, A. P., Crampton, D., & Hutchings, J. B. 1980, ApJ, 241, 269

Domingo, A., Caballero, M. D., Figueras, F., et al. 2003, A&A, 411, L281

Giacconi, R., Murray, S., Gursky, H., et al. 1972, ApJ, 178, 281

Gutiérrez, R., Solano, E., Domingo, A., & García, J. 2004, in Astronomical Society of the Pacific Conference, Vol. 314, Astronomical Data Analysis Software and Systems (ADASS) XIII, 153

Kaper, L., van der Meer, A., & Najarro, F. 2006, A&A, 457, 595

Kuulkers, E., Shaw, S. E., Paizis, A., et al. 2007, A&A, 466, 595

Mas-Hesse, J. M., Giménez, A., Culhane, J. L., et al. 2003, A&A, 411, L261

McNamara, B. J., Harrison, T. E., Zavala, R. T., et al. 2003, AJ, 125, 1437

McNamara, B. J., Norwood, J., Harrison, T. E., et al. 2005, ApJ, 623, 1070

Mendelson, H. & Mazeh, T. 1994, MNRAS, 267, 1

Paredes, J. M., Marziani, P., Marti, J., et al. 1994, A&A, 288, 519

Prince, T. A., Bildsten, L., Chakrabarty, D., Wilson, R. B., & Finger, M. H. 1994, NASA STI/Recon Technical Report N, 95, 30469

Reynolds, A. P., Quaintrell, H., Still, M. D., et al. 1997, MNRAS, 288, 43

Samus, N. N., Durlevich, O. V., Zharova, A. V., et al. 2006, Astronomy Letters, 32, 263

Soldi, S., Walter, R., Eckert, D., et al. 2006, The Astronomer's Telegram, 885, 1

Stover, R. J., Robinson, E. L., Nather, R. E., & Montemayor, T. J. 1980, ApJ, 240, 597

Webster, B. L. & Murdin, P. 1972, Nature, 235, 37

White, N. E., Mason, K. O., Huckle, H. E., Charles, P. A., & Sanford, P. W. 1976, ApJ, 209, L119

Wright, E. L., Gottlieb, E. W., & Liller, W. 1975, ApJ, 200, 171